

Synthesis and Surface Activity of Amphiphilic 2-Acylamido-2-Methylpropane Sulfonic Acid - co-N-Isopropyl Acylamide Nanoparticles in Aqueous Media

Ayman M. Atta¹ and Hussin Al-Shafey²

¹Chemistry department, College of Science, King Saud University, P.O.Box - 2455, Riyadh - 11451, Saudi Arabia.

²Egyptian Petroleum Research Institute, Petroleum Application Department, Nasr City 11727, Cairo, Egypt.

*E-mail: aatta@ksu.edu.sa

Received: 9 February 2013 / Accepted: 3 March 2013 / Published: 1 April 2013

This work is the first report to discuss the effect of nanogels solid particles to lower the surface and interfacial tension of water/air and water/styrene interface. Moreover, this work aims to use nanogels as stabilizer for miniemulsion aqueous polymerization. The present work synthesized a series of amphiphilic crosslinked *N*-isopropylacrylamide (NIPAAm) and 2-acylamido-2-methylpropane sulfonic acid (AMPS) copolymer nanogel based on aqueous copolymerization batch method. In this respect, divinylbenzene (DVB) and N,N-methylene bisacrylamide (MBA) were used as crosslinker. The chemical structure of the prepared nanogels was determined by FTIR analyses. The morphologies of the prepared nanogels were detected by TEM and SEM technique. The lower critical transition temperatures (LCST) were determined from DSC technique. The surface tension of colloidal NIPAm/AMPS dispersions was measured as functions of surface age, temperature, and the morphology of the NIPAm/AMPS nanogels. The NIPAm/AMPS nanogels reduced the surface tension of water to about 30.1 mN/m at 25 °C and a little increase at 40 °C. Surface activities of these nanogels in aqueous water were determined by surface tension measurement. The relationship between surface activity and nanogels morphologies and mol percentages of NIPAm was discussed. The surface adsorption state and surface adsorbed layer of NIPAm/AMPS dispersions were also discussed. Surface parameters such as surface excess concentration (Γ_{\max}), the area per molecule at interface (A_{\min}) and the effectiveness of surface tension reduction were determined from the adsorption isotherms of the prepared surfactants.

Keywords: Surface activity, Amphiphilic nanoparticles, Amphiphilic 2-Acylamido-2-Methylpropane Sulfonic Acid - co-N-Isopropyl Acylamide, aqueous media, mimiemulsion.

1. INTRODUCTION

Much attention has been focused on stable polymeric nanoparticles which have been widely used in drug release system [1], biosensors [2], emulsion and suspension stabilizers [3, 4]. The term nanogel usually refers to a nanoparticle composed of chemically or physically crosslinked synthetic polymers or biopolymers. Nanogels usually have sizes ranging from tens to hundreds of nanometers, with controllable properties, such as swelling, degradation, and chemical functionality [5]. Recently, aqueous ionic polymer micro- and nanogels have received wide attention because of their unique hybrid structure, having cohesive properties of solids and diffusive properties of liquids [6-8]. This is due to their well-defined morphology, size, and surface, as well as to their unique physical and chemical properties [9]. Many different types of solid particles (e.g., naturally occurring or synthetic organic or inorganic particles) behave as surface active materials [10-12]. Ionic nanogels have attracted great interest recently as model systems in colloid science because of their high performance either as polymer or colloid [13-15]. Surface active solid particle offer several advantages over surfactant such as improved surface properties, reduced foaming, and less skin irritation.

Due to the large number of applications in different fields, ranging from nanotechnology to electronics, poly(*N*-isopropylacrylamide) [PNIPAm] is a widely investigated thermoresponsive polymer [16-18]. The amphiphilic nature of PNIPAm attributed to the presence of both amide groups and isopropyl groups, makes it surface active materials [19-21]. PNIPAm-carrying particles behave as surface active materials and adsorb onto an air/water interface [22, 23]. The surface activity of the nanogel particles can be modified by incorporating functional comonomers and/or by changing the nanogel architecture. Their solution properties such as surface charge and colloidal stability strongly depend on the location of the functional groups inside the nanogels [24,25]. Generally, the monodispersed nanogel particles are prepared in the presence or absence of surfactant because of convenient operation [26]. A novel method via a semibatch process in the absence of surfactant has been adopted to prepare nanogels [27]. Based on previous work this article aims to prepare nanogel based on crosslinked *N*-isopropylacrylamide (NIPAm) and 2-acrylamido-2-methylpropane sulfonic acid (AMPS) copolymers using modified technique in the absence of surfactants. Surface activities of these particles in water were determined by surface tension measurement. Also, the relationship between surface activity and molecular structure of the solid particles was discussed. The surface adsorption state and surface adsorbed layer of the amphiphilic nanogels were also discussed. In this respect, the present work is the first report to discuss the effect of nanogels to lowering the surface and interfacial tension.

2. EXPERIMENTAL

2.1. Materials:

N-Isopropylacrylamide (NIPAm) was delivered from Aldrich chemicals Co., recrystallized in toluene : n-hexane (60:40) mixture, and dried. 2-Acrylamido-2-methylpropane sulfonic acid (AMPS), and *N,N*-methylenebis-acrylamide (MBA) were purchased from Merck and recrystallized from acetone and methanol, respectively. Ammonium persulfate (APS) and tetramethylenediamine (TEMED,

99% Aldrich) purchased from Merck and used as initiator. Azobisisobutyronitrile(AIBN), and formamide delivered from Alderich chemical Co. ABIN purified by recrystallizing three times from methanol and drying in vacuum at room temperature.

2.2. Copolymerization of NIPAAm/AMPS:

Crosslinked N-isopropylacrylamide-co-2-acrylamido-2-methylpropane sulfonic acid microgels, NIPAAm/AMPS, were prepared through a modified temperature programmed in the presence of water as a solvent and free surfactant technique. Three different mol ratios of NIPAm (90, 95 and 98 mol %) were used to copolymerize with AMPS monomers. The NIPAAm monomer was dissolved in 40 ml of water and preheated to 40 °C for 30 minute under nitrogen atmosphere. The polymerization process was activated after 5 min with the addition of a catalytic amount of a TEMED solution (0.32 M) dissolved in 5 ml water injected to initiate the polymerization. The temperature of reaction increased up to 55 °C with rate 5 °C per 15 minute. The monomers of NIPAm, AMPS, and MBA were dissolved in 20 ml of water and mixed with APS dissolved in 45 ml of water and then injected with rate 1 ml/minute by means of a syringe pump under stirring. After the feeding was stopped, the reaction temperature increased and kept at 60 °C for 2 hrs. The resultant micro and nanogels were purified by ultracentrifugation at 20000 rpm and the resultant particles were dispersed in water and reprecipitated in 10 fold of acetone.

2.3. Characterization of the prepared surfactants

FTIR spectra were analyzed with a Nicolet FTIR spectrophotometer using KBr in a wavenumber range of 4000–500 cm⁻¹ with a resolution accuracy of 4 cm⁻¹. All samples were ground and mixed with KBr and then pressed to form pellets.

The surface tension measurements of the prepared NIPAAm/AMPS nanogel in water were carried out at different molar concentrations and different temperatures (25 and 45 °C) by using Kruss K-10. The dispersed nanogel solutions gelons were heated in closed bottles using heating thermostat and measured at high temperature for 3 minutes using closed thermostated Kruss K-10 to avoid solvent evaporation.

The surface and interfacial tension measurements between water solution and styrene was measured at 298 K by means of the pendent drop technique using drop shape analyzer model DSA-100 (Kruss, Germany). In this method the shape of a pendent drop is fitted to the theoretical drop profile according to the Laplace equation, using surface tension as one of the adjustable parameters. The error limits of these measurements are on the order of 0.1 mN/m or less. The ADSA-100 analysis required accurate density measurements, which were measured as functions of temperature and nanogels concentration with an AP Par DMA45 MC 1296 densitometer. Pendent drops were formed on the tip of a Teflon capillary with an outside diameter of 0.1 in. and inside diameter of 0.076 in.

SEM images were taken with Gemini microscope DMS-982 (Zeiss, Germany). Samples were prepared in the following manner: 3cm×3 cm aluminium foils were cut and placed on a cleaned glass

plate of size 10cm×10cm then cleaned with dust free tissue paper moistured with acetone. Diluted dispersions of microgel in distilled water (100 μ g/ml) were prepared, sonicated for 5min using Branson sonicator at room temperature and filtered through a 0.45 μ m cellulose acetate filter. The filtrate was placed on the aluminium foil to form a bigger droplet of aqueous dispersion and covered with a glass petri-dish, dried at 37 °C over night. Small pieces of dried films were cut and placed on the SEM sample stage and coated with gold to increase the contrast and quality of the images.

The lower critical solution transition temperature (LCST) behavior of the NIPAAm/AMPS nanogels was determined using DSC. Before the measurement, each sample was dispersed in distilled water at room temperature for 1 hrs and allowed to swell to reach the equilibrium state. Then the swollen sample was placed in a hermetic sample pan and then sealed. The thermal analyses were performed at a heating rate of 5°C/min under a dry nitrogen atmosphere (flow rate of 50 mL/min).

A droplet of the emulsion of St/AMPS was mounted on a glass slide (Matsunami Glass Ind., Ltd.) and examined by using an optical microscope (BX51, Olympus) equipped with a digital camera (XD200, Flovel Co., Ltd.). The size of the emulsion was determined by calculating the average diameter of 50 droplets. Observation at the liquid/liquid interface was carried out with FLVFS-FIS Ver. 1.12 software on a computer.

3. RESULTS AND DISCUSSION

Amphiphilic polyelectrolytes that contain both hydrophobic and electrolyte units on the same polymer chain have received particular attention because they exhibit versatile and yet characteristic properties in aqueous media [28]. These materials are practically important materials for commercial products, such as emulsifiers, solubilizers, suspensifiers, rheology modifiers, and thickeners [29]. Moreover, these materials can be categorized into two classes: one is block, and the other is statistical or random polymers. Block polymers usually form multimolecular micelles with a core-shell structure of well-defined size and shape [30]. The random polymers form a single- or multimolecular micelle in aqueous media, but its structure is much less defined because of the complexity of electrostatic and hydrophobic interactions occurring concurrently along and among the copolymer chains [31]. The micellar structure was characterized in terms of the radius of gyration and density distribution functions of hydrophobic groups, the main chain, and ionic groups as well as of water molecules surrounding the micelle. When an amphiphilic random copolymer is dissolved in water or aqueous salt solution, hydrophobic groups attaching to each copolymer chain tend to self-assemble to form hydrophobic cores, and the copolymer main chain is forced to take the loop conformation. As the result, the amphiphilic random copolymer forms a flower micelle [32]. The present work aims to prepare and copolymerize NIPAm as hydrophobic monomer with AMPS as ionogenic monomer in the presence of MBA as a crosslinker. NIPAm/AMPS microgel was previously prepared in the presence of dodecylbenzene sodium sulfonate (DBSA) as emulsifier at AMPS/NIPAm mol ratio (79.2/18.8) [33]. On the other hand, a series of random copolymers of *N*-isopropylacrylamide (NIPAm) and sodium 2-acrylamido-2-methyl-1-propanesulphonate (AMPS) was synthesized by free radical copolymerization in dimethyl formamide (DMF) as a solvent [34]. The reactivity ratios for the AMPS and NIPAM

monomer, r_{AMPS} and r_{NIPAm} , were 11.0–11.6 and 2.1–2.4, respectively. The values of the reactivity ratios are different from those obtained by Xue et al. who reported that the copolymerization of AMPS and NIPAm in water changes the reactivity ratios to be 2.4 and 0.03 for NIPAm and AMPS, respectively [34]. The values of the reactivity ratios for polar systems are dependent on the solvent effects as a result of association between the radical end of a growing chain and a monomer occurring in its vicinity [35, 36]. The values of the reactivity ratios obtained indicate that the copolymerization is far from azeotropic, and the copolymers obtained should be blocky in nature. In the present study three different crosslinked nanogels with different ratios of NIPAm to AMPS were polymerized in the presence of MBA as crosslinker, TEMED and APS as activator and initiator as represented in the experimental section. The formation of nanogels is based on crosslinking copolymerization of AMP/NIPAm formed by hydrophilic segments covalently attached to a hydrophobic segments are capable of forming a micellar structure as soon as the temperature is raised above their lower critical solution temperature in water. The mechanism of nanoparticles can be discussed on the basis of the formation of NIPAm/acrylic acid microgel particles [37]. On the basis of the studies on the properties of AMPS/NIPAm copolymer gels, it could expect that a small content of AMPS will significantly increase the value of the LCST of NIPAm/AMPS copolymers, due to hydrophilicity of AMPS, up to a complete loss of the temperature-induced transition for the copolymers with a high AMPS content. Therefore, we decided to prepare crosslinked nanogels with a rather low content of AMPS. The reaction mixtures contained 2, 5 and 10 mol % of AMPS, respectively. Accordingly, the proposed synthetic diagram (described in the experimental section) designed to prepare core-shell crosslinked solid nanoparticles. The NIPAm/AMPS nanogels prepared in the presence of semi-interpenetrating PNIPAm polymer network nanoparticles. PNIPAm was first prepared followed by the direct polymerization of AMPS and NIPAAm monomers in a water solution containing cross-linker MBA. In this case, It is expected that, the PNIPAm particles form micellelike aggregates when interact with NIPAm/AMPS, and that the aggregates have much more nanostructures and functionalities.

The FTIR (Figure1) showed absorption bands at 2950, and 2860 cm^{-1} which attributed to the stretching frequency of the aliphatic C-H groups and disappearance of bands at 3000 -3100 cm^{-1} , attributed to CH olefin, which indicated the polymerization of AMPS, NIPAm and MBA. The primary amide carbonyl group peaks of AMPS and NIPAAm units, and secondary amide N-H deformation peaks of microgel units are observed at 1627 and 1545 cm^{-1} , respectively.

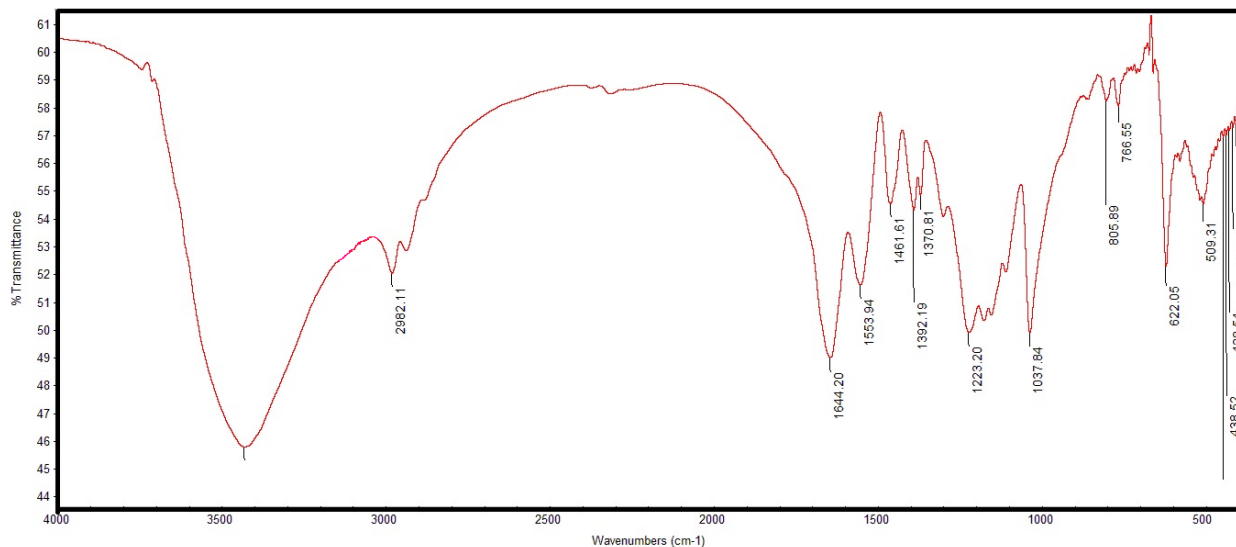


Figure 1. FTIR spectrum of NIPAm/AMPS (98/2 mol %) nanogel.

The peaks at 1465.3 cm^{-1} indicates C-H bending of CH_2 groups, at 1384 cm^{-1} indicating the vibration of the isopropyl group, at 1216 cm^{-1} , 1078 cm^{-1} , and 1016 cm^{-1} re indicating the asymmetric and symmetric stretching of S=O bond of SO_3 groups.

3.1. Morphologies and thermal Characteristics of NIPAm /AMPS nanogels

TEM was used to confirm the morphology of the dispersed and individual NIPAm/AMPS nanogels to elucidate the formation of crosslinked nanoparticles. Figure (2) represented TEM images of NIPAm/AMPS nanogels which showed detailed insight on the morphology of the nanogels. It was proposed that, as the reaction proceeded, the PNIPAm oligomers formed at temperature above LCST at this temperature the crosslinking degree achieved a certain level and the size of the oligomers exceeded the solubility limit, PNIPAm coagulated out of the water phase and formed unstable primary particles. These particles underwent growth and coagulation, thereby increasing the surface charge when polymerized with AMPS, until electrostatic stabilization was achieved. When the hydrophilic monomer, AMPS, was incorporated into the polymerization of NIPAm the coagulation and nucleation were hastened by the hydrogen-bonding interaction between AMPS and NIPAm molecules. The higher AMPS content might be the factors that increased the growth of particles throughout the polymerization process. In this respect, it can be expected that the size of NIPAm/AMPS nanogels, which contain high AMPS content, were larger than the NIPAm/AMPS nanogels contain low AMPS content. However, as expected NIPAm/AMPS nanogels appear dark or with partially transparent, non-uniform periphery which fades towards the boundary (Figure 2a and b). This is because of the higher crosslinked density and complex interlaced structure of NIPAm/AMPS networks.

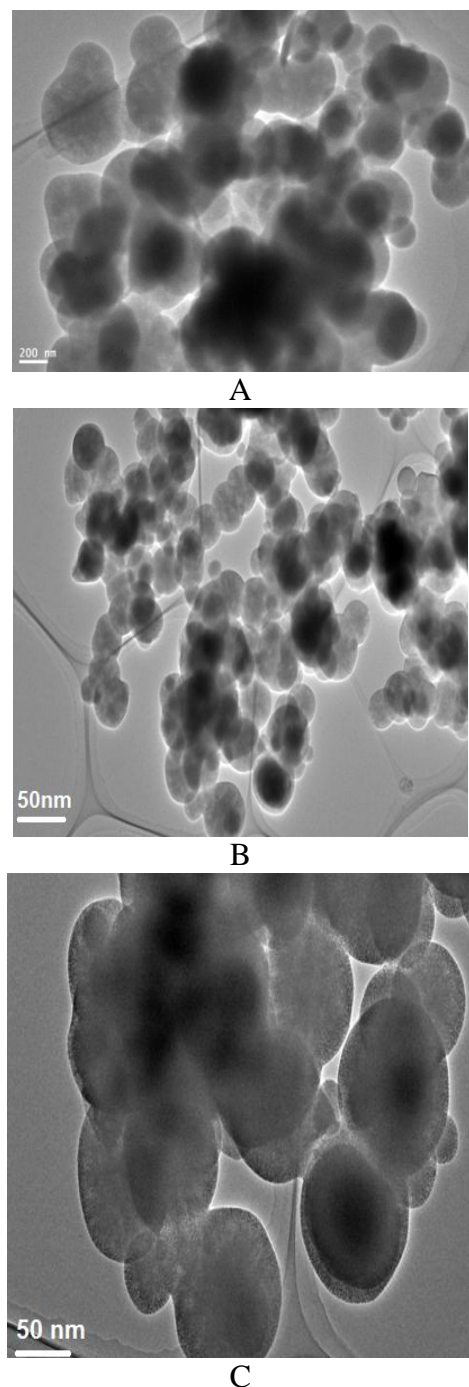


Figure 2. TEM images of NIPAm/AMPS nanogel a)90/10, b) 98/2 and c)95/5 nanogels.

Interestingly NIPAm/AMPS and PNIPAm interpenetrating networks nanogels appear with a smooth, large and completely transparent (fades for a large distance) periphery when the NIPAm content increased NIPAm(98 mol %)/AMPS (2 mol %) (Figure 2c). They spread out completely, because of the hydrated free NIPAm/AMPS chains and the surface was completely transparent and large. It seemed that the NIPAm/AMPS particles showed an obvious core–shell structure with a black core and surrounding shadows, indicating that the nanogels might have an inhomogeneous cross-link density, which gradually decreased from the center to the periphery. TEM analysis indicated that the

average particle diameters ranged from 65 up to 175 nm. The particle size diameters decreased with increasing the NIPAm monomer contents from 90 mol % up to 98 mol % which indicated that the NIPAm monomer plays the important parameters for formation of nanogels as described above. Moreover, it is noticed that NIPAm/AMPS nanogels dried powder is easy to redisperse in distilled water to nanogel solutions. The mean diameter of the nanogels after redispersion shows insignificant change.

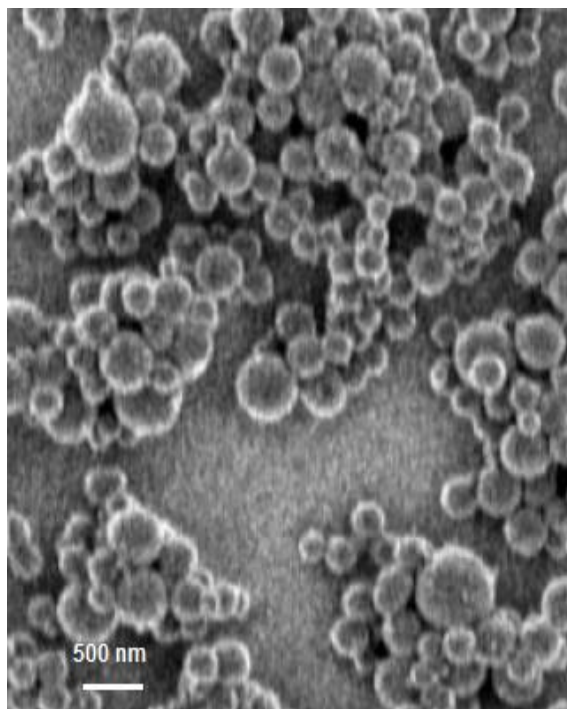


Figure 3. SEM image of NIPAm/AMPS (90/10) nanogel.

Figure 3 shows the SEM image of NIPAm/AMPS (90 mol % / 10 mol %) as representative sample. The particles exhibited relatively smooth spongy spherical morphology which comparable to TEM graphs (Figure 2). The SEM analysis indicates that both NIPAm/AMPS nanoparticles and microparticles occurred during the preparation.

The temperature transitions of the NIPAm/AMPS nanogels were estimated by differential scanning calorimetry (DSC; Figure 4). Wet NIPAm/AMPS nanogel showed two endothermic peaks centered at 32.25, 40.92 °C and 32.15, 42.72 °C for NIPAm/AMPS 95/5 and 90/10 mol%, respectively. The appearance of two peaks indicated the presence of two networks based on PNIPAm and NIPAm/AMPS copolymers with increasing of AMPS mol % content as proposed in the mechanism formation of the nanoparticles. It was also observed that the LCST increased with increase AMPS content due to increase of the nanogel hydrophilicity. NIPAm/AMPS (98/2 mol %) showed one endothermic peak at 35.13 °C. The phase separation has been explained from the viewpoint of entropy effects in the polymer solution [38].

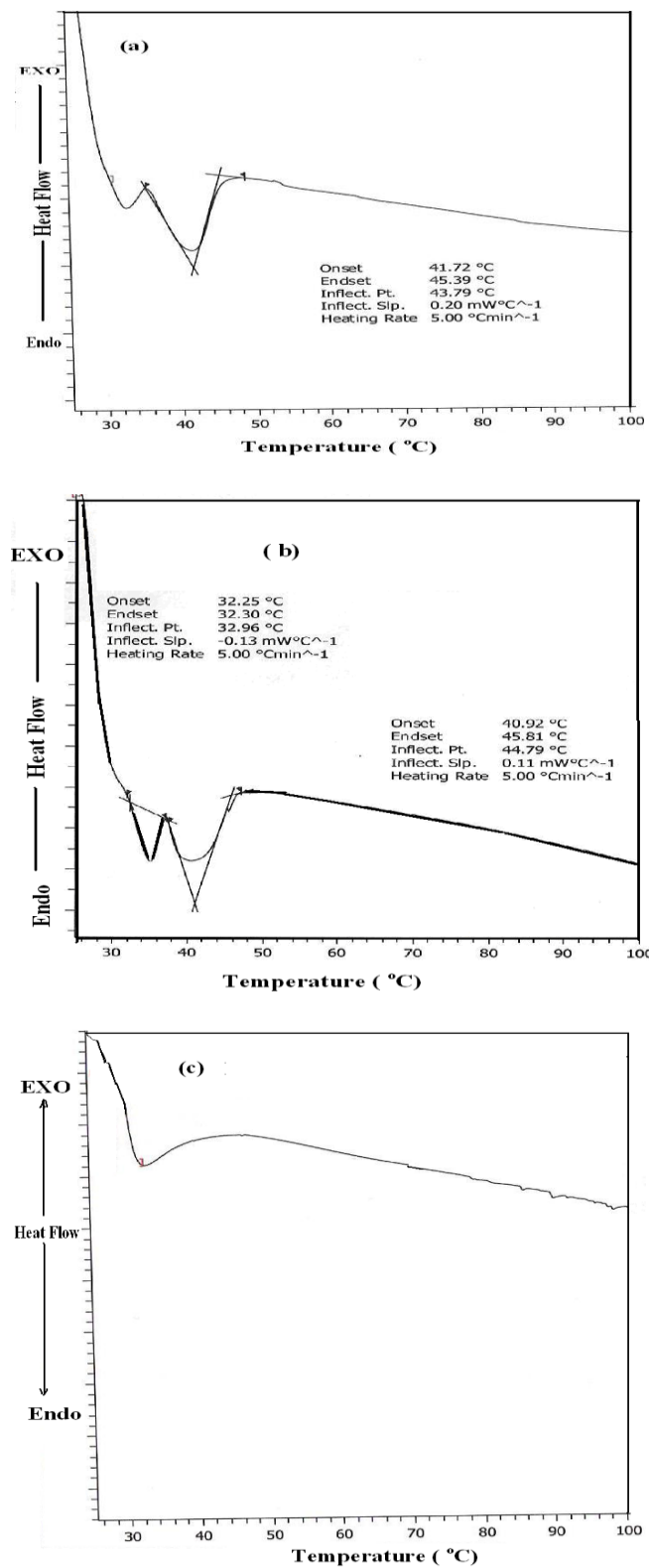


Figure 4. DSC thermograms of NIPAm/AMPS a)90/10, b) 95/5 and c) 98/2 nanogels.

Table 1. LCST characteristics of NIPAm/AMPS nanogels.

Polymer designation	LCST (oC)	ΔH (Jg ⁻¹)	ΔH [kJmol ⁻¹ of NIPAAm unit]
AMPS(2 mol %) / NIPAAm (98 mol %)	35.13	28.2	3.25
AMPS(5 mol %) / NIPAAm (95 mol %)	40.92	23.3	2.77
AMPS(10 mol %) / NIPAAm (90 mol %)	42.72	18.2	2.28

As shown in Table 1, the transition enthalpy of NIPAm / AMPS is somewhat lower than that of PNIPAm [39] because hydration of hydrophobic groups decreases with increasing temperature [38]. Indeed, the mol percent of NIPAm groups in the whole molecule differs among these nanogels. However, a larger fraction of hydrophobic carbon atoms exists in the NIPAm groups. These side groups play a crucial role in the thermosensitive properties of the polymers. Therefore, hydration or dehydration of NIPAm groups before and after the transition might be responsible for the large difference between the transition enthalpies of the nanogels.

3.2. Surface Activity of the NIPAm/AMPS nanogels

Although NIPAm/AMPS microgel was previously prepared in the presence of dodecylbenzene sodium sulfonate (DBSA) as emulsifier at NIPAm / AMPS mol ratio (79.2/18.8) [33] very little is known about their surface activity and interfacial behavior. Although knowledge of surface and interfacial properties is important for application of nanogels and microgels in dispersion and emulsification, not too many publications are dealing with this topic, due to the complexity of describing interfacial and surface properties. The surface tension of colloidal PNIPAm dispersions was measured [40, 41]. It was found that liner PNIPAm could lower the surface tension (γ) of water down to a meso-equilibrium (i.e., the steady-state) value of about 43 mN/m at 25 °C and about 40 mN/m at 40 °C. They reported that, the surface tension did not change much with temperature or molecular weight of PNIPAm. It was also reported that, the incorporation of more hydrophilic acrylamide groups gave higher surface tension values [42]. In the present work, the dynamic surface tension of the three nanogels samples of NIPAm/AMPS were measured at water/air interface by variation nanogels concentrations and temperature of measurements from 25 to 45 °C. The relation between the surface tension and time at different nanogels concentrations were represented in figure 5 as representative samples. The relation between the surface tension and concentrations (-ln c; mol/L) of nanogels at 25 and 45 °C was illustrated in figure 6. The data illustrated in figure 5 indicated the surfactants reached the equilibrium after different time intervals when the concentration lowered than 0.16 mol/L (2 Wt %). Furthermore, the time scales for surface tension lowering were much longer at lower nanogels concentrations and high temperature (45 °C) where the nanogels were shrunken. These data proved that the prepared NIPAm/AMPS nanogels highly adsorbed at air/water interface at concentration of 0.16 mol/L (2 Wt %). On the other hand the data of the surface tension indicated the prepared

NIPAm/AMPS nanogels reduced the water surface tension, from 72.7 to 30.1 mN/m, with lowering the nanogel concentration.

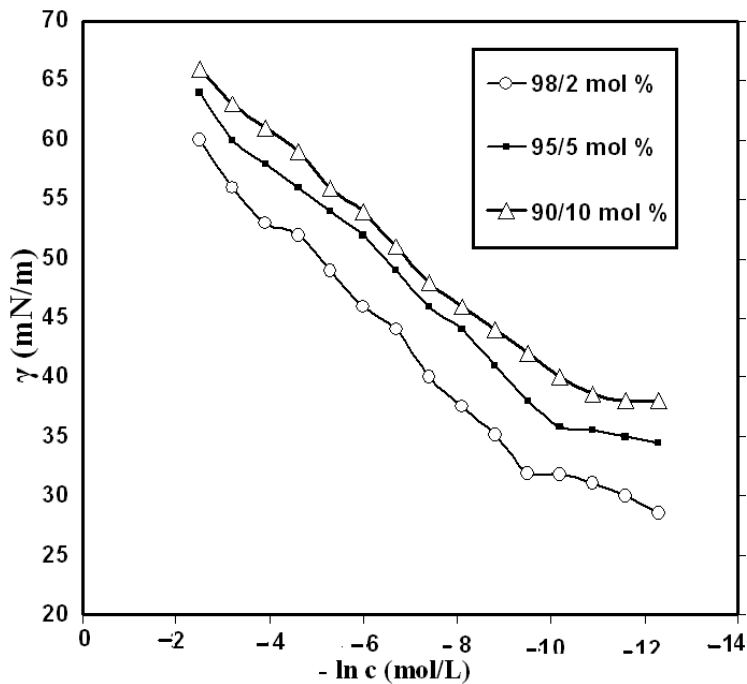


Figure 5. Adsorption isotherms of NIPAm/AMPS nanogel at 25 °C.

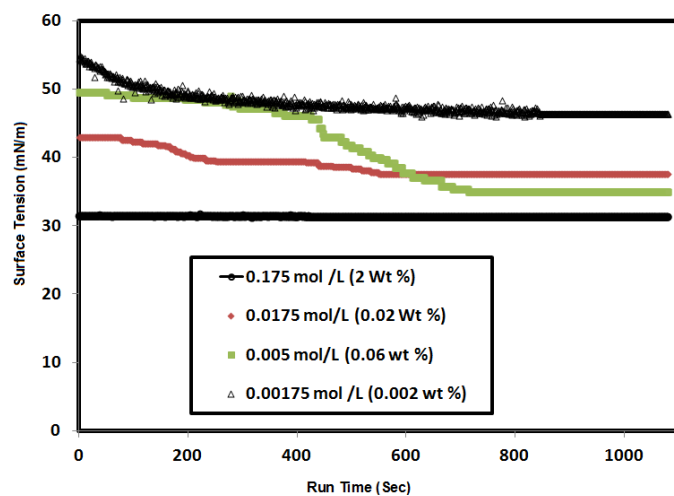


Figure 6. Surface tension relation with time for different concentrations of NIPAm/AMPS (98/2 mol %) at 25 °C.

Moreover, it was found that the prepared nanogels behave like surfactant when dispersed and adsorbed at water solution and air/water interface, respectively. It is well known that, the micellization or aggregation are therefore an alternative mechanism for adsorption of the surfactant at the interfaces

for removing the lipophobic groups from contact with the solvent, thereby reducing the free energy of the system. The micellization, aggregation and adsorption of surfactants are based on the critical micelle and critical aggregation concentrations (cac), which were determined by the surface balance method as represented in figure 6. The cac values of the prepared NIPAm/AMPS nanogels surfactants were determined in water at 25 and 45 °C from the change in the slope of the plotted data of surface tension (γ) versus the solute concentration ($\ln C$) and listed in table 2.

The intersection in the surface tension curves can be used to determine cac values of the prepared NIPAm/AMPS nanogels and the corresponding surface tension is defined as γ_{cac} . The effectiveness of the NIPAm/AMPS nanogels was expressed by the maximum reduction of surface tension of the organic solvents which calculated from the equation, $\Delta\gamma = \gamma_{\text{water}} - \gamma_{\text{cac}}$. The $\Delta\gamma$ values of the prepared NIPAm/AMPS nanogels were determined and listed in Table 2. It was observed that clear dispersant solutions were obtained for the NIPAm/AMPS nanogels in water without precipitation even at 5 Wt % of the surfactant concentrations which indicated the good dispersion of the NIPAm/AMPS nanogels. The differences in surface activity of surfactants are based on the high adsorption of a high concentration of NIPAm/AMPS nanogels at the air/water interface.

Table 2. Surface properties of the NIPAm /AMPS nanogels at different temperatures.

Designation NIPAm /AMPS	Temp. (°C)	cac mol/L	γ_{cac} mN/m	$\Delta\gamma$ mN/m	$(-\partial\gamma/\partial\ln c)$	$\Gamma_{\max} \times 10^{10}$ mol/ cm ²	A_{\min} nm ² /molecule
90/10	25	0.012	37.2	35.0	4.03	1.62	0.102
	45	0.007	35.8	33.1	4.58	1.68	0.096
95/5	25	0.009	34.2	28.0	5.03	2.03	0.082
	45	0.005	32.8	36.1	5.46	2.07	0.080
98/2	25	0.006	30.1	43.1	5.8	2.26	0.069
	45	0.003	33.4	35.4	5.4	2.18	0.076

A possible explanation seems reasonable to propose that surface tension data involves two processes the adsorption of nanogels to the interface and the unfolding of surface tails and loops to cover the entire interface. Furthermore, it is expected the adsorption in a quiescent drop to be influenced by the size of the nanogel (i.e., smaller is faster) whereas the unfolding should be determined by the mobility of individual chain segments in the gel, which in turn is influenced by crosslinking and water content[40]. In this respect, the data of TEM (figure 2) and DSC (figure 4) indicated that NIPAm/AMPS (98/2 mol%) has uniform network and smaller particle size which be able to adsorb at interface and has the ability to reduce the surface tension more than NIPAm/AMPS (90/10 mol%) nanogels which agree with the data of surface activity listed in Table 2. The data indicated the surface tension increased with increasing the temperature for both NIPAm/AMPS (90/10 mol%) and (95/5 mol%). While NIPAm/AMPS (98/2 mol%) shows lower surface tension with increase It was expected that, at high temperature the viscosity of water is lower and the diameters of

the nanogels are less due to gel collapsed, so transport to the surface should be faster [40]. In the present system NIPAm/AMPS (90/10 mol%) and (95/5 mol%) nanogels had the greatest content of PNIPAm networks, as illustrated in DSC and TEM, because of non-uniform morphology of these nanogels more quickly spread over the surface at 25 °C. By contrast at 40 °C the PNIPAm networks are collapsed on the nanogels structure and adsorption is slower. It demonstrates the tremendous effect of temperature on the nanogel-covered interface. The pendent drop reaches a regular shape and trans from opaque to transparent upon cooling, indicating that the nanogels are able to rearrange at the interface as compared to the packing at 25 °C.

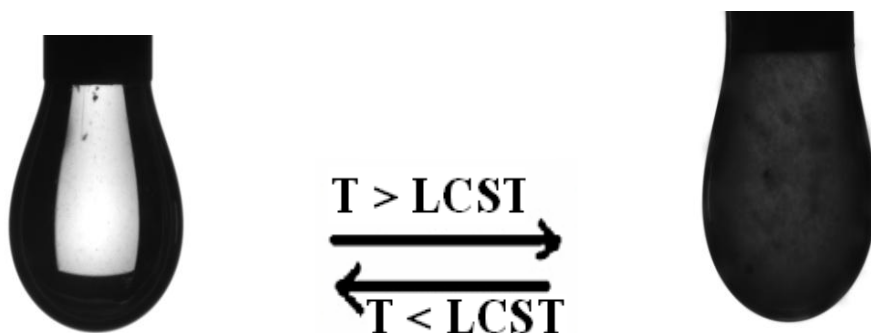


Figure 7. Effect of Temperature on drop opacity of (0.175 mol / L) NIPAm/AMPS (98/2)nanogel.

Figure 7 shows a picture of a pendent drop, which was prepared at 25 °C and 45 °C. The sensitivity of pendant drop to change from opaque to transparent drop up on heating and cooling was decreased with increasing of AMPS contents from 2 to 10 mol%. This behavior indicated that, the softness and deformability of the nanogels are also temperature- dependent.

The amount of NIPAm/AMPS nanogels adsorbed per unit area of liquid–gas or liquid–liquid interface, although possible, is not generally undertaken because of the difficulty of isolating the interfacial region from the bulk phase for purposes of analysis when the interfacial region is small, and of measuring the interfacial area when it is large. The orientation and packing of NIPAm/AMPS nanogels molecules at the air/water interface prominently depend upon the molecular structure, and extent of association of the nanogels and solvent molecules as described in the previous section. In this respect, the amount of NIPAm/AMPS nanogels adsorbed per unit area of interface is calculated indirectly from the surface or interfacial tension measurements. The concentration of NIPAm/AMPS nanogels at the solvent–air interface can be calculated as surface excess concentration Γ_{\max} . The surface excess concentration of NIPAm/AMPS nanogels at the interface can be calculated from surface or interfacial tension data using the following equation: $\Gamma_{\max} = 1/RT \times (-\partial \gamma / \partial \ln c)_T$, where $(-\partial \gamma / \partial \ln c)_T$ is the slope of the plot of γ versus $\ln c$ at constant temperature (T) and R is the gas constant (in $J \text{ mol}^{-1} \text{ K}^{-1}$). The surface excess concentration at surface saturation is a useful measure of the effectiveness of adsorption of NIPAm/AMPS nanogels at the liquid–gas or liquid–liquid interface, since it is the maximum value that adsorption can attain. The Γ_{\max} values were used for calculating the minimum area A_{\min} at the aqueous–air interface. The area per molecule at the interface provides

information on the degree of packing and the orientation of the adsorbed NIPAm/AMPS nanogels, when compared with the dimensions of the molecule as obtained from models. From the surface excess concentration, the area per molecule at the interface is calculated using the equation: $A_{\min} = 10^{16}/N \Gamma_{\max}$, where N is Avogadro's number. The data of Γ_{\max} , A_{\min} , and $(-\partial \gamma / \partial \ln c)$ were determined and listed in Table 2. As shown in Table 2, A larger Γ_{\max} means that more NIPAm/AMPS nanogel molecules adsorbed on the surface of the solution, which also means a lower surface tension. The lowest value of A_{\min} obtained is $0.069 \text{ nm}^2/\text{molecule}$ suggests adsorption of NIPAm/AMPS nanogel with PNIPAm chain which oriented away from the liquid in a more tilted position. However, a low A_{\min} data suggest compact adsorption of NIPAm/AMPS chains at interface or complete surface coverage by a NIPAm/AMPS rigid film, even though the AMPS chains are oriented at the liquid surface. Careful inspection of data, Table 2, indicates those, A_{\min} of the NIPAm/AMPS have two opposite relations with the temperature. The A_{\min} decreased with increasing the temperature. This can be attributed to fact that the A_{\min} decreased at the surface as a result of enhanced molecular motion of the NIPAm/AMPS at higher temperature [43]. One possible explanation is that the terminal location of the AMPS group allows the NIPAm/AMPS molecules to adapt a flexible loop-like conformation on the interface [43].

4. CONCLUSIONS

1. Amphiphilic crosslinked NIPAm/AMPS nanogel prepared with spherical morphology using surfactant free polymerization.
2. NIPAm/AMPS and PNIPAm interpenetrating networks nanogels appear with a smooth, large and completely transparent (fades for a large distance) periphery when the NIPAm content increased NIPAm(98 mol %)/AMPS (2 mol %).
3. The appearance of two peaks in DSC thermograms indicated the presence of two networks based on PNIPAm and NIPAm/AMPS copolymers with increasing of AMPS mol % content as proposed in the mechanism formation of the nanoparticles.
4. NIPAm/AMPS nanogels adsorb at the air/water interface and lower the surface tension of water.
5. The orientation and packing of NIPAm/AMPS nanogels molecules at the air/water interface prominently depend upon the molecular structure, and extent of association of the nanogels with water.

ACKNOWLEDGMENT

The project was supported by the research center college of science, King Saud University

References

1. M. Motornov, Y. Roiter, I. Tokarev, S. Minko, *Progress Polymer Science* 35 (2010)174-211.
2. J. Kim, M. Serpe, L. A. Lyon, *Journal American Chemical Society* 126 (2004) 9512-9513.

3. B. Brugger, B. Rosen, W. Richtering, *Langmuir* 24 (2008) 12202-12208.
4. M-A. Trojer, K. Holmberg, M. Nydén, *Langmuir* 28 (2012) 4047-4050.
5. H. Hayashi, M. Iijima, K. Kataoka, Y. Nagasaki, *Macromolecules* 37 (2004) 5389-5396.
6. L. Sannier, R. Bouchet, M. Rosso, J.-M. Tarascon, *Journal Power Sources*, 158 (2006) 564-570.
7. M. Stephan , *European Journal Polymer* 42 (2006) 21-42.
8. Z. Li , M-H. Kwok, T. Ngai, *Macromolecular Rapid Communication* 33 (2012) 419-425.
9. D. C. Sundberg, Y. G. Durant, *Polymer Reactive Engineering*, 11 (2003) 379-432.
10. B. P. Binks, *Current Opinion Colloid Interface Science* 7 (2002) 21-41.
11. R. Aveyard, B. P. Binks, J. H. Clint, *Advanced Colloidal Interface Science* 100–102(2003) 503-546.
12. J. T. Russell, Y. Lin, A. Böker, L. Su, P. Carl, H. Zettl, J. He, K. Sill, R. Tangirala, T. Emrick, K. Littrell, P. Thiagarajan, D. Cookson, A. Fery, Q. Wang, T. P. Russell, *Angewandte Chemie International Edition* 44 (2005) 2420-2426.
13. H. Senff, W. Richtering, *Journal Chemistry Physics* 111 (1999) 1705-1711.
14. M. Stieger, J. S. Pedersen, P. Lindner, W. Richtering, *Langmuir* 20 (2004) 7283-7292 .
15. L. A. Lyon, A. Fernandez-Nieves, *Annual Review of Physical Chemistry* 63 (2011) 2.1-2.19.
16. D. Durancher, *Langmuir* 16,(2000) 9002-9008.
17. Z. M. O. Rzaev, S. Dincer, E. Pikan, *Progress Polymer Science* 32 (2007) 534-595.
18. R. R. Schmidt, R. Pamies, A. L. Kjoniksen, K. Zhu, J. G. Hernandez Cifre, B. Nystrom, J. Garcia de la Torre, *Journal Physical Chemistry B* 114 (2010) 8887-8893.
19. M. Kawaguchi, W. Saito, T. Kato, *Macromolecules* 27 (1994) 5882-5884.
20. J. Zhang, R. Pelton, *Langmuir* 12 (1996) 2611-2612.
21. M. Kawaguchi, Y. Hirose, T. Kato, *Langmuir* 12 (1996) 3523-3526.
22. K. Chan, R. Pelton, J. Zhang, *Langmuir* 15 (11) (1999) 4018-4020.
23. S. Tsuji, H. Kawaguchi, *Langmuir* 24 (2008) 3300-3305.
24. T. Hoare, R. F. Pelton, *Langmuir* 20 (2004) 2123-2133.
25. P. Sheikholeslami, C. M. Ewaschuk, S. U. Ahmed, B. A. Greenlay, T. Hoare, *Colloid Polymer Science* 290 (2012) 1181-1192.
26. G. Huang, Z. Hu, *Macromolecules* 40 (2007) 3749-3756.
27. Q. Zhang, L. Zha, J. Maa, B. Lianga, *Journal Colloid Interface Science* 330 (2009) 330-336.
28. C. L. McCormick, J. Bock, D. N. Schulz, In *Encyclopedia of Polymer Science and Engineering*, Kroschwitz J. I., Ed.; Wiley & Sons: New York, Vol. 17 (1989) 730-784.
29. J. E. Glass, Ed. *Associative Polymers in Aqueous Solutions*; ACS Symposium Series 765; American Chemical Society: Washington, DC, 2000.
30. S. Forster, V. Abetz, A. H. E. Muller, *Advanced Polymer Science* 166 (2004) 173-210.
31. A. Hashidzume, Y. Morishima, K. Szczubialka, In *Handbook of Polyelectrolytes and Their Applications*, S. K. Tripathy , J. Kumar , H. S. Nalwa, Eds.; American Scientific Publishers: Stevenson Ranch, CA, 2, (2002) 1-63.
32. Y. Tominaga, M. Mizuse, A. Hashidzume, Y. Morishima, T. Sato, *Journal Physical Chemistry B*, 114 (2010) 11403–11408.
33. M. Miyake, K. Ogawa, E. Kokufuta, *Langmuir* 22(2006) 7335-7341.
34. K. Szczubialka, R. Losaka, M. Nowakowska, *Journal Polymer Science Part A: Polymer Chemistry* 39 (2001) 2784-2792.
35. W. Xue, S. Champ, M. B. Huglin, *Polymer* 41 (2000) 7575-7581.
36. H. J. Harwood, *Makromolecular Chemistry Macromolecular Symposium*, 10/11(1987) 331-354.
37. C-L. Lin, W-Y. Chiu, C-F. Lee, *Journal Polymer Science: Part A: Polymer Chemistry*, 44 (2006) 356-370.
38. H. Feil, Y. H. Bae, J. Feijen, S.W. Kim, *Macromolecules* 26 (1993) 2496-2500.
39. Y. Haba, C. Kojima, A. Harada, K. Kono, *Angewandte Chemie* 119 (2007) 238-241.
40. J. Zhang, R. Pelton, *Langmuir* 15(1999) 8032-8036.

41. J. Zhang, R. Pelton, *Colloids Surfaces A*, 156 (1999)111-122.
42. J. Zhang, R. Pelton, *Journal Polymer Science Part A: Polymer Chemistry* 37(1999) 2137-2143.
43. X. J. Xu, H. L. Goh, K. S. Siow, L. M. Gan, *Langmuir* 17 (2001) 6077-6085.